THE
PHYSICAL REVIEW

A journal of experimental and theoretical physics established by E. L. Nichols in 1893

SECOND SERIES, VOL. 88, No. 3 NOVEMBER 1, 1952

Elastic Scattering of 10-Mev Deuterons by H^3 and He^3*

J. C. ALLRED, A. H. ARMSTRONG, A. M. HUDSON, R. M. POTTER, E. S. ROBINSON, LOUIS ROSEN, AND E. J. STOVALL, JR.
University of California, Los Alamos Scientific Laboratory, Los Alamos, New Mexico
(Received July 16, 1952)

The d-t and d-He^3 differential elastic scattering cross sections have been measured for the 10-Mev deuteron bombarding energy of the external beam of the Los Alamos cyclotron. Nuclear plates detected the charged particles in the angular region 30° to 140° in the c.m. coordinate system. Although the cross section as a function of angle shows marked asymmetries, indicative of scattering contributions from partial waves of high angular momentum, the two curves are identical above 45° in the c.m. system.

I. INTRODUCTION

THE scattering of light nuclei is, in itself, an important method for studying the nature of nuclear forces. However, aside from the general interest in interactions between light nuclei, there is additional importance attached to the pair of interactions d-t and d-He^3 because the respective compound nuclei differ only by one unit of charge. It was therefore anticipated that an accurate determination of the differential elastic scattering cross sections for the above reactions would provide information concerning the equality of n-n and p-p forces.

There already exists an imposing amount of evidence which points to the equality of n-n, p-p, and n-p forces. This evidence may be briefly summarized as follows:

(a) It is possible to calculate the mass differences of mirror nuclei which undergo radioactive transitions from a knowledge of the electrostatic energies of the nuclei and the n-p mass difference.[1–5] This suggests that the strictly nuclear forces among a group of nucleons are not influenced, if neutrons are replaced by protons and vice versa.

(b) Further evidence for the equality of n-n and p-p forces is to be found in the almost linear variation of nuclear binding energies as a function of atomic weight.[6]

(c) Finally, the equivalence of n-n and p-p forces has been inferred from experiments on n-d and p-d scattering.[7] Also, analysis of p-p scattering has shown the ^1S wave interactions between neutron-proton and proton-proton to be approximately equal if ranges and potential shapes are assumed identical except for a small difference in potential depth.[8] This, however, can be accounted for by the magnetic interaction between nucleons, if a Yukawa potential is postulated.[9,10] Although, until recently, it appeared that interpretation of the results of the high energy scattering experiments required postulating inequality of p-p and n-p forces,[11] these data can now be explained by introduction of a spin orbit interaction which is velocity dependent,[12] or by a very short-range repulsive force.[13]

The interactions $d+t \rightarrow He^4+n$ and $d+He^3 \rightarrow He^4+H^1$ have been investigated at this laboratory for 10-Mev deuterons[14,15] with the result that, within experimental error, the differential cross sections are found to be identical. It is, however, questionable whether these results can be cited as evidence for the equality of n-n and p-p forces since it may be that these results can be satisfactorily explained by a stripping theory.[16,17] However,

* Work performed under the auspices of the AEC.

[1] Fowler, Delsasso, and Lauritsen, Phys. Rev. **49**, 561 (1936).
[2] White, Delsasso, Fox, and Creutz. Phys. Rev. **56**, 512 (1939).
[3] White, Creutz. Delsasso, and Wilson, Phys. Rev. **59**, 63 (1941).
[4] L. D. P. King and D. R. Eliot, Phys. Rev. **58**, 846 (1940) and **59**, 403 (1941).
[5] Brown, Snyder, Fowler, and Lauritsen, Phys. Rev. **82**, 159 (1951).
[6] L. A. Young, Phys. Rev. **48**, 913 (1935).
[7] Gregory Breit, Phys. Rev. **80**, 1110 (1950).
[8] Breit, Condon, and Present, Phys. Rev. **50**, 825 (1936).
[9] Breit, Hoisington, Shore, and Thaxton, Phys. Rev. **55**, 1103 (1939).
[10] J. Schwinger, Phys. Rev. **78**, 135 (1950).
[11] R. S. Christian and E. W. Hart, Phys. Rev. **77**, 441 (1950).
[12] K. M. Case and A. Pais, Phys. Rev. **80**, 203 (1950).
[13] R. Jastrow, Phys. Rev. **79**, 389 (1950).
[14] Brolley, Fowler, and Stovall, Phys. Rev. **82**, 502 (1951).
[15] J. C. Allred, Phys. Rev. **84**, 695 (1951).
[16] S. T. Butler, Proc. Roy. Soc. (London) **A208**, 559 (1951).
[17] S. T. Butler and J. L. Symonds, Phys. Rev. **83**, 858 (1951).

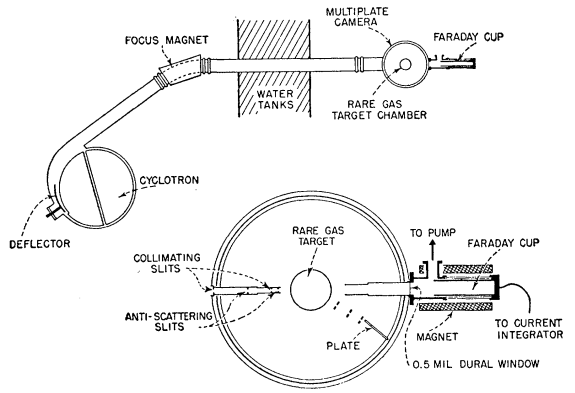

FIG. 1. Experimental geometry, showing details of mounting Faraday cup at rear of multiplate camera.

the similarity (or dissimilarity) of the differential d-t and d-He^3 elastic scattering cross section may well be more amenable to interpretation on the basis of the charge independence of nuclear forces.

II. EXPERIMENTAL ARRANGEMENT

The Los Alamos cyclotron and focusing magnet provided a well-collimated beam of 10-Mev deuterons at a distance of 15 feet from the cyclotron tank and 4 feet from the water walls. A nuclear multiple plate camera was aligned with its axis coincident with the axis of the deuteron beam. At the center of the camera was placed a thin-walled target chamber which served to confine the He^3 and tritium gases. The nuclear plate detectors were arranged behind slit systems and around the periphery of the camera in such a way that each plate could "see" an accurately defined section of the reaction volume. The angular resolution of the slit systems through which the reaction particles passed was $\pm 0.8°$. The angular divergence of the incident deuteron beam was 0.85° in the vertical direction and 1.2° in the horizontal direction. After traversing the 0.5-mil Duraluminum window of the nuclear plate camera, those deuterons scattered through large angles by the window were removed by an additional collimating system built into the camera. This collimating system permitted a maximum angular divergence of $\pm 2°$. Data on the range and intensity distributions of the reaction products were taken over the laboratory angular interval 15° to 115°.

A detailed description of the method for utilizing the cyclotron beam and of the design and construction of the camera are given elsewhere.[18,19]

In an experiment where small amounts of rare gases are used, as in the case in the present experiment, the advantages of nuclear emulsions as detectors are significant. In the first place, they make possible the rapid acquisition of data over a large angular region. Since these data are obtained simultaneously at angular intervals of 2.5°, one can derive accurate relative cross-sectional values from a single run and for the same set of cyclotron conditions. The second significant advantage is to be found in the ability to discriminate between real and spurious counts by means of the orientation and range of the tracks in the detectors. This is quite important when one is obliged to use a target chamber to confine the scattering gas, since the chamber itself becomes a scatterer and one must discriminate against particles which suffer such scattering.

The experimental details and procedure for making cross-sectional measurements with our nuclear multiplate camera were altered somewhat for the present experiment from that previously described.[20] The changes in the experimental arrangement are illustrated in Figs. 1 and 2. The target gases were contained in a hollow cylinder with a 0.5-mil Duraluminum window around its periphery. This target chamber was made by slotting a hollow Duraluminum cylinder over a region encompassing 300° and then covering the slotted section with 0.5-mil Duraluminum foil. The foil was sandwiched between the above cylinder and a second cylindrical shell, which was slotted and machined to fit snugly around the main cylinder in such a way that the two slotted sections overlapped. The outer shell and foil were then arc-welded to the inner cylinder, the welding being done in a argon atmosphere. A target chamber prepared in the above manner can hold a positive pressure of approximately one atmosphere. In case of window failure during a run, the gas would have been confined by the camera and could have been recovered. However, no target window failures occurred while He^3 or tritium were contained.

The charge measurement was carried out as previously described[20] with the exception that the Faraday cup was attached to the camera proper so as to obviate the necessity for placing the camera and Faraday cup in another vacuum system. The Faraday cup had its own pumping system and was evacuated to a pressure less than 10^{-5} mm Hg before each run.

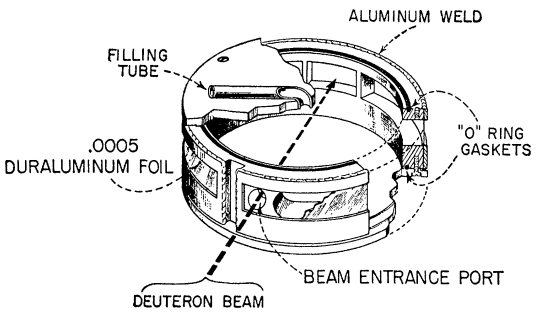

FIG. 2. Cutaway drawing of rare gas target chamber.

[18] Curtis, Fowler, and Rosen, Rev. Sci. Instr. **20**, 388 (1949).
[19] Allred, Rosen, Tallmadge, and Williams, Rev. Sci. Instr. **22**, 191 (1951).
[20] L. Rosen and J. C. Allred, Phys. Rev. **82**, 777 (1951).

III. PURIFICATION AND HANDLING OF GASES

The beta-decay of tritium permits the preparation of an isotopically pure He^3 sample. A sample of tritium (in this case 95 percent H^3, 5 percent H^1) reacted with finely divided and out-gassed uranium to form UH_3. The decay rate of the tritum is about 0.5 atomic percent per month. Since He^3 has a monatomic molecule, the volume growth of He^3 is about one percent per month. The He^3 gas used in the present experiment was obtained in this manner. Additional purification of the He^3 is done by passing the gas sample over activated charcoal at liquid air temperature.

The physical properties of UH_3 make the purification of the tritium sample quite convenient. At room temperature the pressure of tritium over UH_3 with an excess of uranium is $\sim 10^{-5}$ mm Hg. Thus one can remove any gaseous contaminant by pumping on the UH_3 at room temperature with a mercury diffusion pump. Moderate heating evolves the hydrogen isotopes, which are admitted to the target chamber at the desired pressure. Finely divided uranium is an excellent getter; hence, traces of water vapor or oxygen are readily removed by the heated uranium.

Since the rate of evolution of the tritium-hydrogen mixture is somewhat variable, an auxiliary expansion volume, V_1 of Fig. 3, is used in the initial stage of target filling. The volume of the system comprising the uranium furnace, V_1, and the manometer leads was arranged so as to be approximately that of the Dural gas target chamber inside the camera. Gas is initially evolved to about twice the desired pressure in the filling system. The uranium furnace is then closed off from the system, and the gas is admitted to the target chamber. This procedure eliminates the possibility of target window breakage by gas surges from the uranium furnace.

After the target gas has come to temperature equilibrium with the target chamber and filling system, the bombardment is begun. At the conclusion of the run. the tritium-hydrogen mixture is recovered in the uranium furnace. When the furnace is reconnected to the target chamber, the tritium-hydrogen pressure drops rapidly to a value of the order of 10^{-5} mm Hg at room temperature.

He^3 gas is stored in the container V_2. A sufficient quantity is used to fill the target chamber to the desired pressure by expansion. The gas is recovered in V_2 by means of the Toepler pump shown in Fig. 3. A two-way stopcock is provided at the top of the Toepler pump for use in the He^3 fillings.

The pressure is measured by reading the manometer with a good cathetometer. The temperature is taken as room temperature, which is the same as the temperature of the body of the nuclear plate camera. The temperature and pressure readings are taken after the gas has come to temperature equilibrium in the target, as evidenced by the stability of the pressure reading. The

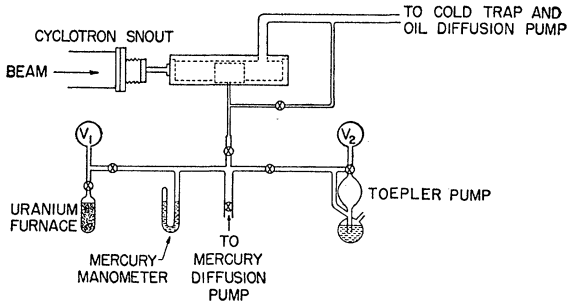

FIG. 3. Gas system for filling the rare gas target with H^3 and He^3 and recovering the samples after running.

atomic density, n_0, in atoms/cm^3, is calculated from

$$n_0 = nPAT_0 d / P_0(T_0+t)V_0,$$

where n = number of atoms per molecule of target gas; P = pressure of gas in target; A = Avogadro's number = 6.025×10^{23} molecules/mole; T_0 = standard temperature = 273°K; P_0 = standard pressure = 76.0 cm Hg; t = room temperature in °C; V_0 = molar volume at STP = 2.24×10^4 cm^3; d = (density of Hg at temperature t)/(density of Hg at 0°C).

IV. EXPERIMENTAL PROCEDURE

The procedure for making a run is as follows:

The multi-plate camera is loaded with nuclear plates (Ilford C-2), the emulsion thickness chosen being such that the highest range particles to be observed will be stopped within the emulsion. The camera and target chamber are then pumped down by means of an oil diffusion pump to a pressure less than 10^{-4} mm Hg. Simultaneously, the Faraday cup is pumped down by its own oil diffusion system to a pressure less than 10^{-5} mm Hg. At this time the current integrator is calibrated,[20] after which the target chamber is disconnected from the camera and both are closed off from the pumping system. Tests are now made with He^4 to determine whether the target chamber is completely tight at a pressure significantly higher than the pressure to be used in the run. If the chamber does not leak, the scattering gas is introduced into it in the manner described in Sec. III. The pressure of the gas is now observed until temperature equilibrium is attained with the target chamber and camera, as evidenced by the constancy of the pressure. During this time the cyclotron is warmed up and an internal beam obtained. After the final pressure measurement the deflector is energized, and a beam of 0.05 to 0.3 μa is passed through the target for a time ranging from 3 to 15 minutes. This accomplished, the pressure in the target is remeasured and the gas reclaimed. If H^3 is used as the target gas, the camera is pumped down by means of a fore pump vented to an outdoor stack as a precaution against traces of H^3 gas which might have found their way into the camera. The last step involves opening the camera to the air for removal of plates.

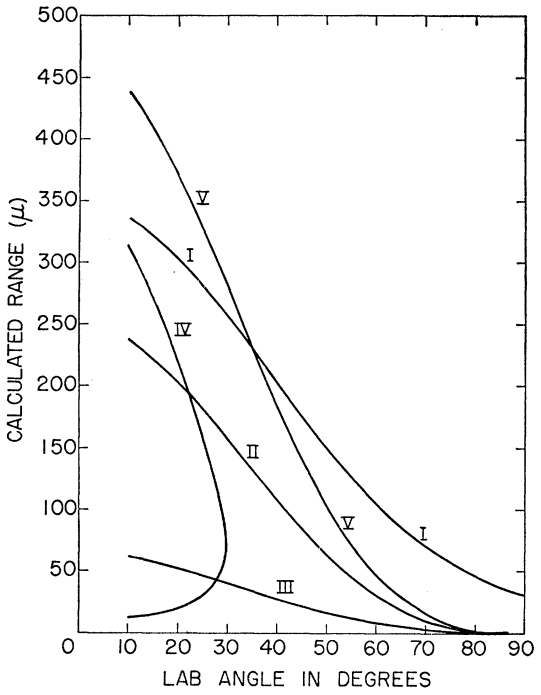

FIG. 4. Range *versus* angle for the scattering interactions of 10-Mev deuterons with protons, tritons, and He^3 nuclei. I. deuterons scattered by H^3 or Hd^3; II. recoil tritons; III. recoil He^3 nuclei; IV. deuterons scattered by H^1; V. recoil protons.

In order to make an over-all check on the accuracy with which we might expect to make absolute cross-sectional measurements under the new conditions of containing the target gas and mounting the Faraday cup, we ran experiments on *d-p* and *d-d* scattering. Both of these reactions have been investigated with high accuracy[20–23] and under more favorable conditions than could now be employed. The gases were introduced in precisely the same manner as was to be used for the H^3 and He^3. The results of these runs show that, although the target walls are responsible for a considerable number of background tracks, the error introduced by background at angles above 20° in the laboratory system is quite small. Above this angle, the cross sections obtained for *d-p* and *d-d* elastic scattering agree to within 3 percent with previous measurements. This result gave us confidence that we were measuring current correctly, and that the 0.5-mil Duraluminum target window was not producing spurious effects by way of multiple small angle scattering of the reaction particles.

V. ANALYSIS OF PLATES

The precedure for analyzing the plates is the same as has been previously described.[20] The analysis of each plate starts with a determination of the distribution in range of the charged particles recorded in one or more swaths of the plate. Each swath is approximately 100 microns wide and 3 cm long. Since elastic scattering processes yield monoergic groups of particles, it is immediately possible from energy considerations to identify each group of tracks with the corresponding reaction product. Having made this identification, one counts the tracks falling within the desired range groupings over a sufficient number of swaths to give the statistical accuracy desired. The range analysis makes possible discrimination against all tracks not due to elastic scattering and, in the case of tritium, those due to deuterons scattered by hydrogen contamination in the tritium as well as hydrogen nuclei projected by the deuterons. Protons from the $d+He^3 \rightarrow He^4+p$ reaction are of sufficiently high energy as to cause no confusion. He^4 particles from the $d+t \rightarrow He^4+n$ reaction are of sufficiently low energy so that they also cause no difficulty. Neither of the above reactions has a sufficiently high cross section to add significantly to the track density on the plates.

The range distribution of the various reaction particles recorded can be anticipated on the basis of energy and momentum considerations and the appropriate range-energy relationships for the nuclear emulsion used. Let E_D = incident deuteron energy; E_1 = energy of deuteron scattered by a mass 3 particle; E_2 = energy of projected mass 3 particle; E_3 = energy of deuteron scattered by a proton; E_4 = energy of projected proton; E_5 = maximum energy of proton for reaction disintegration of the deuteron upon collision with either a triton of a He^3; Q = binding enregy of deuteron = −2.2 Mev; θ = angle which scattered deuteron makes with incident deuteron direction: ϕ = angle which projected particle (He^3, H^3, or H^1) makes with incident deuteron direction. Then

$$E_1=(4/25)E_D\{\cos\theta+[(9/4)-\sin^2\theta]^{\frac{1}{2}}\}^2; \quad (1)$$

$$E_2=(24/25)E_D\cos^2\phi; \quad (2)$$

$$E_3=(4/9)E_D\{\cos\theta\pm[(1/4)-\sin^2\theta]^{\frac{1}{2}}\}^2; \quad (3)$$

$$E_4=(8/9)E_D\cos^2\phi; \quad (4)$$

$$E_5=(2/25)E_D\{\cos\phi+[6+10(Q/E_D)-\sin^2\phi]^{\frac{1}{2}}\}^2. \quad (5)$$

Each energy may now be converted into a range in Ilford C-2 nuclear emulsions by use of the appropriate range-energy relationship.[24] Figure 4 gives the variation of range in Ilford C-2 emulsions with angle for the various reaction particles from the processes with which we are concerned and for an incident deuteron energy of 10 Mev.

The energy of the incident deuteron beam was determined from the ranges in Ilford C-2 emulsions of the elastically scattered deuterons on either side of the incident beam direction, and the above-mentioned range-energy curves. Account was taken of energy losses by the scattered deuterons in the target gas and in the

[21] Mather, Karr, and Bondelid, Phys. Rev. **78**, 292 (1950).
[22] Rodgers, Leiter, and Kruger. Phys. Rev. **78**, 656 (1950).
[23] Allred, Erickson, Fowler, and Stovall, Phys. Rev. **76**, 1430 (1949).
[24] J. Rotblat, Nature **167**, 550 (1951).

target chamber window. The incident beam energy for the present experiments was determined to be 10.3 ±0.2 Mev.

It is apparent from the range-energy curves that, at least in principle, it is possible to resolve the various groups of particles present in each reaction over most of the angular region in which measurements can be made. The greatest difficulty arises from H^1 contamination in the H^3. However, since the cross section for d-p scattering is accurately known at the energy in question, it is possible to determine the amount of H^1 contamination in the tritium. This is done by counting tracks in the proton peak from *d-p* scattering at angles where this peak is well resolved from the deuteron and triton peaks. By this means we determined that our H^3 sample contained 5.5 atomic percent H^1 impurity. It was then possible to correct for the H^1 contamination at angles where we did not have adequate resolution to separate the reaction products from *d-p* scattering from those arising from *d-t* scattering by using the derived value of H^1 impurity and the known cross section for *d-p* scattering.

Figure 5 shows the range distribution of the charged particles at various angles for *d-t* and *d*-He^3 interactions. The identity of the particles responsible for the various groups is inferred from Fig. 4. The reaction products enter the surface of the plate at a grazing angle of 11.8° and the plotted ranges of Fig. 5 are projected ranges, rather than absolute ranges.

From an inspection of the range distributions in Fig. 5, it is apparent that a good deal of "background" is present. This background introduces considerable inaccuracy in making absolute cross-sectional measurements on the elastic processes, since it is difficult to determine precisely just how much background is included within the range limits of a given group of particles. The background correction was made by drawing in the background on the basis of its magnitude on either side of the particle group in question in such a way that the peak went to zero on both sides. The widths of the resultant peaks were required to be consistent with the widths calculated from homogeneity of the beam, angular resolution, and range straggling.

VI. CORRECTIONS AND EVALUATION OF ERRORS

As indicated above, it is necessary to make corrections for background and hydrogen contamination in the H^3. The correction for H^1 contamination amounts to as much as 20 percent in some cases, due to the relatively large *d-p* cross section as compared to *d-t*. However, in most cases, this correction is no more than 10 percent and can be made quite precisely. The correction for other background, including protons from deuteron disintegration, is also as much as 20 percent in the worst cases and this produces considerable inaccuracy in the final results.

The errors involved in the absolute elastic scattering cross sections were evaluated as follows: geometry, ±1 percent; background, ±0–20 percent; charge measurement, ±1.5 percent; microscope calibration, ±0.5 percent; personal errors, ±1 percent; statistics, ±2–3 percent. Errors were evaluated separately for each angle at which a cross-sectional measurement was made.

Runs were made at pressures of 0.7 to 9.2 cm Hg and with integrated currents of 2.9 to 69.6 μcoulombs. The results were self-consistent within the inaccuracies imposed by statistics and background. The fact that widely different gas pressures and currents yielded the same cross-sectional values is convincing evidence that serious errors do not arise due to background from multiple scattering in the target gas, or from scattering by the slits and target windows. It is also evidence that our current measurement was not influenced by the target gas and that our pressure measurements were self-consistent.

VII. RESULTS AND DISCUSSION

Table I and Fig. 6 give the data obtained for the elastic scattering cross section as a function of angle in the c.m. system.

There is unmistakable evidence (see Fig. 5) for deuteron disintegration in both the *d-t* and *d*-He^3 interactions. It is also apparent that deuterons on He^3 produce more disintegrations than deuterons on H^3.

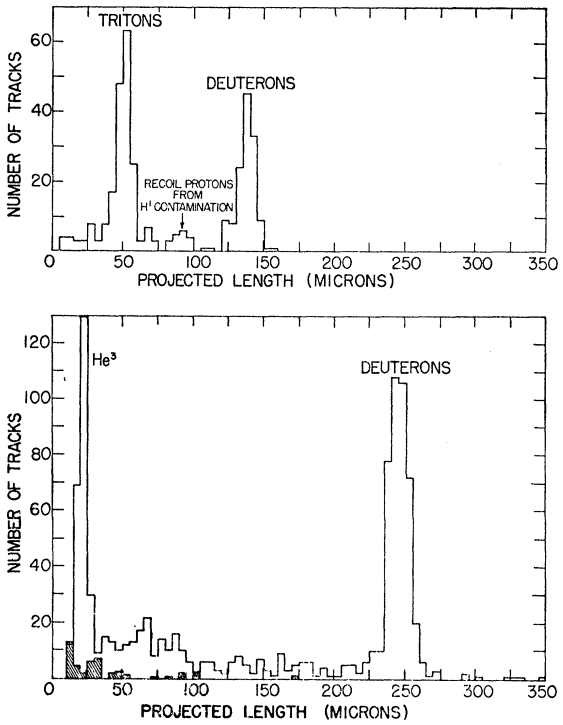

FIG. 5. Range distributions observed for the interaction of 10.2-Mev deuterons with tritium (above) and He^3 (below). The laboratory angles of observation are 50° and 30°, respectively. The shaded area in the lower histogram indicates the result of a background run made without gas in the target. The results are normalized to integrated beam current and plate area analyzed.

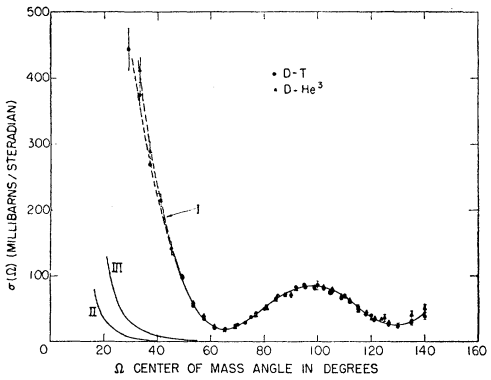

FIG. 6. Differential cross section *versus* center-of-mass angle for *d-t* and *d*-He³ elastic scattering; II. calculated Coulomb scattering for *d-t*; III. calculated Coulomb scattering for *d*-He³. $E_D=10.2$ Mev.

A least squares analysis of the variation with angle of the differential elastic cross section for *d-t* and *d*-He³ scattering gives the following result:

$$\sigma(\Omega)=0.0790-0.1013\cos\Omega-0.3776\cos^2\Omega+0.3111\cos^3\Omega+0.7601\cos^4\Omega+0.0929\cos^5\Omega+0.0800\cos^6\Omega.$$

This indicates that at least D waves, and possibly F waves, are effective in the scattering processes.

Above 45° c.m., where Coulomb scattering is small compared to nuclear scattering, the *d-t* and *d*-He³ differential cross sections for elastic scattering appear to be identical within the accuracy of the present experiments. If one assumes the charge independence of nuclear forces, then one might anticipate that, for large scattering angles, the two differential cross sections should also be identical provided all other factors are equal. The factors to be considered are the difference in electrostatic energies of the compound nuclei, the difference in magnetic energies, and, perhaps most important, the difference in potential barriers for the incoming and outgoing deuteron.

The difference in magnetic energies is negligibly small. The difference in electrostatic energies should be approximately that between H³ and He³. This is given by the difference of the *n-p* mass difference and the beta-ray end-point energy in the decay of H³ to He³.

TABLE I. Differential cross sections as a function of center-of-mass angle for *d-t* and *d*-He³ scattering at 10.2-Mev bombarding energy

Ω degrees	*d-t* $\sigma(\Omega)$ barns	*d*-He³ $\sigma(\Omega)$ barns
29.1	0.444 ±0.028	
33.2	0.374 ±0.017	0.418 ±0.019
37.3	0.268 ±0.012	0.290 ±0.013
41.4	0.216 ±0.010	0.215 ±0.011
45.4		0.142 ±0.007
49.5	0.0968±0.0045	0.100 ±0.005
53.5	0.0559±0.0031	0.0597±0.0029
57.5	0.0362±0.0023	0.0391±0.0021
61.4	0.0221±0.0013	0.0240±0.0016
65.4	0.0200±0.0015	0.0183±0.0013
69.3	0.0252±0.0013	0.0235±0.0012
70.0	0.0258±0.0015	
73.1	0.0298±0.0016	0.0295±0.0014
75.0	0.0383±0.0022	
76.9	0.0456±0.0022	0.0404±0.0019
80.0	0.0503±0.0025	
80.7	0.0567±0.0028	0.0515±0.0024
84.4	0.0662±0.0036	0.0639±0.0031
85.0	0.0705±0.0033	
88.1	0.0732±0.0038	0.0721±0.0033
90.0	0.0724±0.0035	
91.7	0.0838±0.0041	0.0804±0.0039
95.0	0.0870±0.0043	
95.3	0.0852±0.0040	0.0861±0.0040
98.8	0.0834±0.0042	0.0837±0.0039
100.0	0.0861±0.0040	
102.2	0.0818±0.0040	0.0843±0.0040
105.0	0.0763±0.0036	0.0768±0.0038
105.5	0.0780±0.0039	0.0814±0.0043
108.8	0.0682±0.0032	0.0696±0.0033
110.0	0.0705±0.0034	0.0695±0.0033
112.0	0.0609±0.0033	0.0642±0.0031
115.0	0.0529±0.0026	0.0478±0.0032
115.1	0.0546±0.0027	0.0532±0.0045
118.1	0.0433±0.0023	0.0452±0.0026
120.0	0.0403±0.0020	0.0356±0.0020
121.0	0.0348±0.0016	0.0364±0.0029
123.9		0.0347±0.0054
125.0		0.0362±0.0051
126.6	0.0268±0.0013	0.0300±0.0034
130.0		0.0246±0.0021
135.0	0.0300±0.0033	0.0409±0.0050
140.0	0.0392±0.0044	0.0538±0.0076

Its value is 764 kev,[25] which is quite small compared to the excitation energy.

The difference in Coulomb barriers in the two cases is approximately 0.25 Mev. In the center-of-mass system, the energy available is about 6 Mev, which is large compared to the highest Coulomb barrier (~0.5 Mev for *d*-He³).

[25] Taschek, Jarvis, Argo, and Hemmendinger, Phys. Rev. **75**, 1268 (1949).